Marine and Petroleum Geology 122 (2020) 104635

Contents lists available at ScienceDirect

Marine and Petroleum Geology

journal homepage: www.elsevier.com/locate/marpetgeo

Review article

A compilation of igneous rock volumes at volcanic passive continental margins from interpreted seismic profiles

Molly M. Gallahue [a,*], Seth Stein [a], Carol A. Stein [b], Donna Jurdy [a], Mitchell Barklage [a], Tyrone O. Rooney [c]

[a] Department of Earth and Planetary Sciences, Northwestern University, 2145 Sheridan Rd., Evanston, IL, 60208, USA
[b] Department of Earth and Environmental Sciences, University of Illinois at Chicago, Chicago, IL, 60607-7059, USA
[c] Department of Geological Sciences, Michigan State University, East Lansing, MI, 48824, USA

ARTICLE INFO

Keywords:
Volcanic passive margins
Seaward dipping reflectors
High velocity lower crust

ABSTRACT

The rifting and breakup of continents, and subsequent seafloor spreading, give rise to passive continental margins, many of which are underlain by enormous volumes of igneous rocks and termed volcanic passive margins. The relationships between the igneous rocks, rifting, and mantle plumes remain unresolved despite extensive studies and proposed alternative models. To support such studies, we use published, previously interpreted, seismic reflection and refraction data to compile a dataset of igneous rock volumes and geometries at volcanic passive continental margins. The VOLMIR (VOLcanic passive Margin Igneous Rocks) dataset is based on margin-crossing profiles on which the volumes and geometries of both shallow seaward dipping reflector (SDR) and deeper high velocity lower crustal (HVLC) units can be measured. It includes information about the ages of continental breakup, and profile distances from the associated Euler pole and from hotspots that may have played roles in the breakup process. Despite local variations, the dataset shows general patterns. The average ratio of SDR to HVLC volumes, ~0.3–0.4, is relatively consistent between profiles, implying that formation of these units is related during continental breakup. The volumes of igneous rocks display a moderate positive correlation with distances from the Euler pole, but only a weak negative correlation with distances from the nearest hotspot (at the time of margin formation), suggesting that in continental breakup lithospheric processes (passive rifting) have greater effects than hotspots (active rifting). These results suggest that this dataset will be useful for exploring aspects of the rifting process, relationships between volcanic rifted margins, and potential explanations for their similarities and differences.

1. Introduction

The rifting and breakup of continents, and subsequent seafloor spreading, give rise to passive continental margins, zones of transition between continental and oceanic portions of the same plate (Fig. 1). The formation of these margins can be divided into three stages: 1) rifting, in which crustal stretching occurs, 2) breakup, in which the crust and mantle rupture, and 3) drifting (seafloor spreading) in which continental crust on either side continues to diverge as oceanic crust forms in between (Huismans and Beaumont, 2011; Busby and Azor Pérez, 2012; Norcliffe et al., 2018; Alves et al., 2020). These stages are defined in various related but different ways. For example, breakup is defined by Harkin et al. (2020) as the rupture and separation of continental crust and lithosphere, by Geoffroy et al. (2015) as when the integrated strength of the rifting lithosphere drops to zero, and by Bronner et al. (2011) as ending when seafloor spreading begins. Thus the stages can overlap, illustrating the complexities involved. For example, faulting and earthquakes along the East African rift show that the crust retains finite strength down to 30 km (Shudofsky et al., 1987). GPS data show that the distinct Nubian and Somalian plates on either side are moving apart (Saria et al., 2013), although seafloor spreading has not yet started, as it has along the other two arms (Gulf of Aden and Red Sea) of the three-plate (Nubia-Somalia-Arabia) system (Zwaan et al., 2020).

Seismic reflection and refraction studies show that most rifted margins are underlain by enormous volumes of igneous rocks resulting from extensive magmatism during rifting and breakup, and are thus termed volcanic, or magma-rich margins (Roberts and Bally, 2012; Franke, 2013). Hence volcanic passive margins are generally considered to be

* Corresponding author.
E-mail address: molly@earth.northwestern.edu (M.M. Gallahue).

https://doi.org/10.1016/j.marpetgeo.2020.104635
Received 31 March 2020; Received in revised form 29 July 2020; Accepted 1 August 2020
Available online 11 August 2020

Large Igneous Provinces (LIPs) (Eldholm and Grue, 1994). These typically formed where continental breakup was associated with the eruption of continental flood basalts, dikes, and sills during prerift and/or synrift stages of continental separation, in which large-scale melting gave rise to thick igneous units (Menzies et al., 2002). This process is often hypothesized to involve mantle plumes (e.g., Dewey and Burke, 1974), although this hypothesis remains controversial (Foulger and Jurdy, 2007).

However, the details on the relationship between rifting and breakup, igneous units, and mantle plumes remain unclear despite extensive observational and modeling studies (Menzies et al., 2002; Mjelde et al., 2002; Geoffroy, 2005; Faleide et al., 2008; Blaich et al., 2011; Franke, 2013; Biari et al., 2017). A useful tool for such studies would be a global dataset of volcanic passive margin properties that could be employed to identify similarities and differences, and thus explore their causes. Accordingly, we use seismic reflection and refraction data along previously published and interpreted profiles across magma-rich (volcanic) passive continental margins to compile a dataset of igneous rock volumes. The dataset also includes information about the tectonics of these margins' formation, namely the ages of breakup, volcanism, and initiation of seafloor spreading, proximities to the Euler pole associated with rifting and distance from hotspots that may have influenced the rifting process.

2. Volcanic units

Seismic surveys show that volcanic passive margins have a characteristic general architecture, with local variations (e.g., Eldholm and Grue, 1994; Geoffroy, 2005; Schnabel et al., 2008; Koopmann et al., 2014) (Fig. 2). Heavily intruded and thinned continental crust, transitional between continental and oceanic crust, is overlain by seaward dipping reflectors (SDRs), which result from packages of volcanic flows interbedded with volcaniclastic sediments and tuffs (e.g., McDermott et al., 2018). The high-amplitude reflections are thought to result from interference between closely spaced flows (Planke and Eldholm, 1994). SDRs form throughout the rifting-breakup-initial seafloor spreading sequence (Soares et al., 2012; Alves and Cunha, 2018; Alves et al., 2020; Harkin et al., 2020). Although most SDRs occur landward of the oldest oceanic crust, yielding large magnetic anomalies landward of the oldest seafloor spreading anomalies (Davis et al., 2018), some SDRs occur above oceanic crust. The transitional crust and in some cases oldest oceanic crust are underlain by a high velocity lower crustal (HVLC) unit (e.g., Menzies et al., 2002; Blaich et al., 2011; Franke, 2013; Eddy et al., 2014). Because volcanic passive margins and nonvolcanic passive margins (passive margins lacking extensive breakup-associated magmatism)

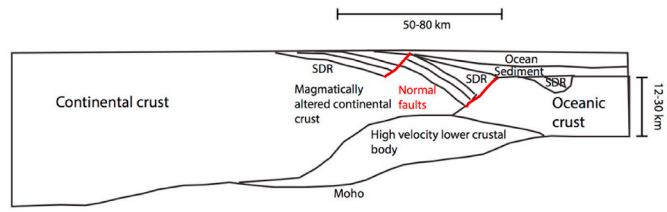

Fig. 2. Simple schematic cross section through a rifted volcanic passive margin, showing characteristic tectonic elements, after Geoffroy (2005).

are end members of a spectrum (Franke, 2013), some margins may fall between the end members. For our purposes, a margin is considered volcanic if it contains evidence of an SDR unit on a previously interpreted seismic profile.

Because various authors use different nomenclature in interpreting their profiles, we adopt criteria for consistent characterization.

SDRs are seaward dipping reflector units, typically wedge-shaped thickening seaward, located at or near the continent-ocean boundary (Mutter and Detrick, 1984; Menzies et al., 2002; Franke, 2013; Geissler et al., 2017; Tugend et al., 2018). SDRs can be up to 10–20 km thick, extend oceanward for tens to hundreds of kilometers, and extend along margins for hundreds to thousands of kilometers (McDermott et al., 2018; Norcliffe et al., 2018; Tian and Buck, 2019). Drill core analyses find that SDRs consist of interbedded thick basaltic flows and thin sediment deposits (e.g., White et al., 1987; Geoffroy, 2005; McDermott et al., 2018; Paton et al., 2017; Tian and Buck, 2019). They are thought to have erupted in subaerial or shallow marine environments (e.g., White et al., 1987; Geissler et al., 2017).

In compiling VOLMIR, SDRs were defined as units satisfying several of the following descriptors:

1. Wedges of seaward dipping reflectors that thicken oceanward, often with high seismic reflection amplitudes, on or near the continent-ocean boundary.
2. The reflectors may be horizontal at their farthest landward extent, but can dip up to 20° or more seaward, or have a concave down (convex up) curvature.
3. Interbedded basaltic material, sediments, volcaniclastic deposits, volcanic tuff, and/or hyaloclastite.
4. Formation at the time of continental rifting, breakup, or initial seafloor spreading.
5. Extend oceanward tens to hundreds of kilometers, along-margin for hundreds to thousands of kilometers, and up to 10–20 km thick.

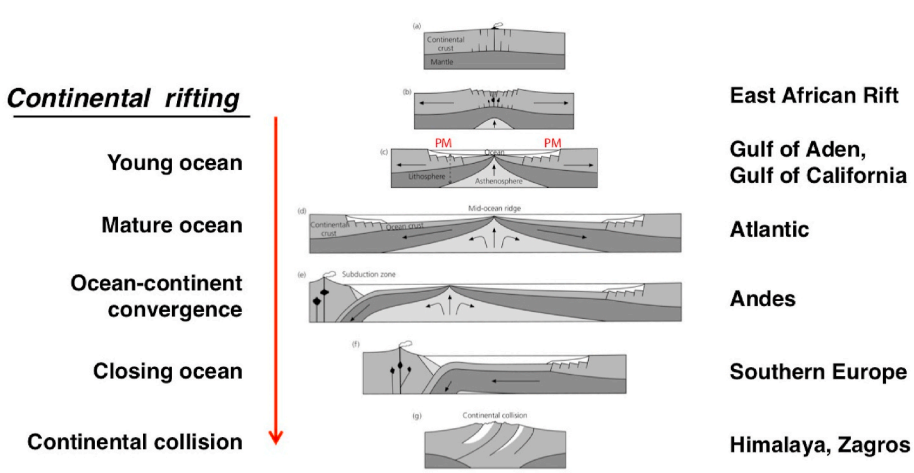

Fig. 1. Schematic illustration of the Wilson cycle, showing modern areas at each stage (Stein and Wysession, 2003). Passive margins, denoted by "PM", form by continental rifting and breakup followed by initial seafloor spreading that forms a young ocean basin.

HVLC units are observed on many seismic profiles as thick units, far below the SDRs, with an unusually high P-wave velocity (White et al., 1987; Keen et al., 1987; Tréhu et al., 1989; Diebold et al., 1988; Austin et al., 1990; Sheridan et al., 1993; Menzies et al., 2002; Blaich et al., 2011; Franke, 2013). Their P-wave velocities range between 7.2 and 7.7 km/s, significantly higher than the typical velocity of oceanic crust, ~6.4–6.6 km/s (Geoffroy, 2005). Due to the depth of HVLCs, they are not directly sampled by drilling, so their exact nature is unknown. However, modeling of the gravity signatures and other analyses find that a magmatic HVLC best fits the data (Holbrook and Kelemen, 1993; Kelemen and Holbrook, 1995; Mjelde et al., 2002; Becker et al., 2014; Paton et al., 2017). HVLCs are up to 25 km thick (Kelemen and Holbrook, 1995; Menzies et al., 2002).

In VOLMIR, HVLCs are defined as units satisfying several of the following:

1. A body with seismic velocities from 7.2 to 7.7 km/s.
2. Up to 25 km thick, above the Moho and typically below SDRs.
3. Thought to be magmatic in origin with formation at the time of continental breakup.
4. Located between continental and oceanic crust.

3. VOLMIR dataset

Fig. 3 illustrates how SDR and HVLC units were classified on previously published and interpreted seismic profiles by the scheme listed above. Units' boundaries were digitized and their cross-sectional areas projected in the extension direction were measured using the publicly available Java image analysis program ImageJ (Schneider et al., 2012) (https://imagej.net/Welcome).

Profile locations are shown in Fig. 4. Although the profiles give two-dimensional cross-sectional areas of units, we assume the areas are proportional to volumes in adjacent regions. Comparisons between nearby profiles support this assumption (Fig. 4). The dataset is based preferentially on margin-crossing profiles on which the volumes (i.e. cross-sectional areas) of both shallow SDR and deeper HVLC units can be measured. We also used some profiles on which SDR volumes could be assessed, even if the HVLC volumes could not.

We consider the sum of SDR and HVLC volumes on a profile to be the total rift-related igneous material on the profile. This approximation neglects the volume of intrusions into thinned continental crust, which we have no good way to assess. For most of our analyses, this choice has little effect because we compare volumes between profiles rather than absolute volumes. Because HVLC units typically lie at considerable depth and thus can be difficult to resolve on the seismic lines, the minimum requirement for inclusion in the VOLMIR dataset (and classification as a volcanic passive margin) is the presence of SDRs. Due to uncertainties in measuring volumes of buried material, the volumes should be considered approximations to highlight general patterns rather than precise measurements.

Margin profiles used in the dataset, publication source, units and classification criteria are listed in Table 1. The measured volumes of SDR, HVLC, and total igneous units are given in Table 2.

For Atlantic Ocean margins, the dataset also includes information about the ages of continental breakup, proximity from Euler pole associated with rifting, and distance from hotspots that may have played roles in the rifting (Tables 3 and 4). The locations at time of rift formation of the associated Euler pole and hotspots were obtained from PALEOMAP_GlobalRotationModel_19a.rot and 07hotspotsv15a3.gmpl, respectively, in the GPlates software documentation (Müller et al., 2018) (www.gplates.org).

4. Results

Despite the uncertainties in all stages of the compilation process, including local variations in structure and the challenge of combining seismic sections acquired and processed differently, we find that useful patterns emerge.

4.1. Average volumes of igneous units

For the profiles, the average SDR volume is 372 km^2 and the average HVLC volume is 844 km^2. A histogram of SDR volumes (Fig. 5) shows five outliers at one standard deviation. These outliers (Transect 3 Namibia – 949 km^2, Walvis – 1100 km^2, Pelotas South – 1526 km^2, Luderitz – 1808 km^2, and Punta del Este – 2356 km^2) have SDR volumes of 900 km^2 and greater. The average volume excluding these outliers is 217 km^2 with a median of 185 km^2.

The outliers are from the South Atlantic and appear as high total volcanic volume lines in Fig. 4. These margins are thought to have been affected by the Tristan de Cunha hotspot which formed the Rio Grande and Walvis Rises on the South American and Nubian plates (Gladczenko et al., 1998; Blaich et al., 2011; Reuber and Mann, 2019). Possibly, this hotspot contributed more melt to the margins, resulting in higher SDR volumes than at other margins. The Paraná-Etendeka continental flood basalts (LIPs) of South America and Africa are also considered to have formed as a result of the Tristan de Cunha hotspot at the time of rifting between the continents, further supporting the view that the hotspot produced significant melt (Reuber and Mann, 2019).

4.2. Ratio of igneous units

We observe a relatively consistent ratio of SDR to HVLC volumes between profiles (Fig. 6). The median ratio is 0.29, indicating that SDR volumes are approximately 29% that of HVLC. The mean ratio, 0.38, is skewed high by two outliers.

The first outlier, with a ratio of 1.55, is the Transect 3 line located off the coast of Namibia (Gladczenko et al., 1998). This line has poor resolution at depths below ~15 km, so we interpret the high ratio as due to incomplete imaging of the full HVLC unit. The second outlier, with a

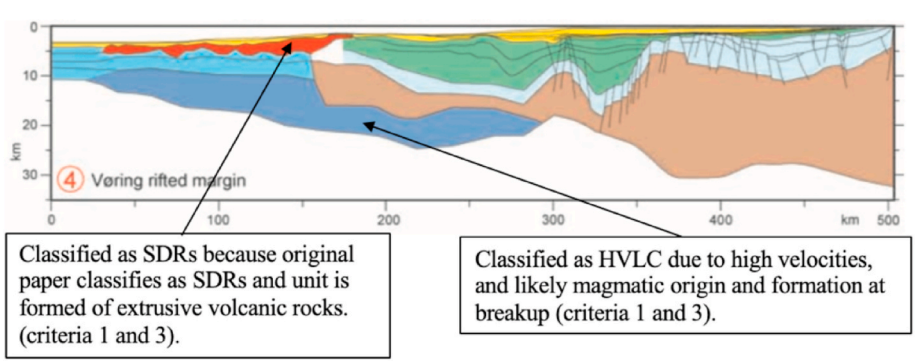

Fig. 3. Vøring 4 profile (Faleide et al., 2008) (Table 1) illustrating SDR and HVLC unit classifications, via criteria listed in the text.

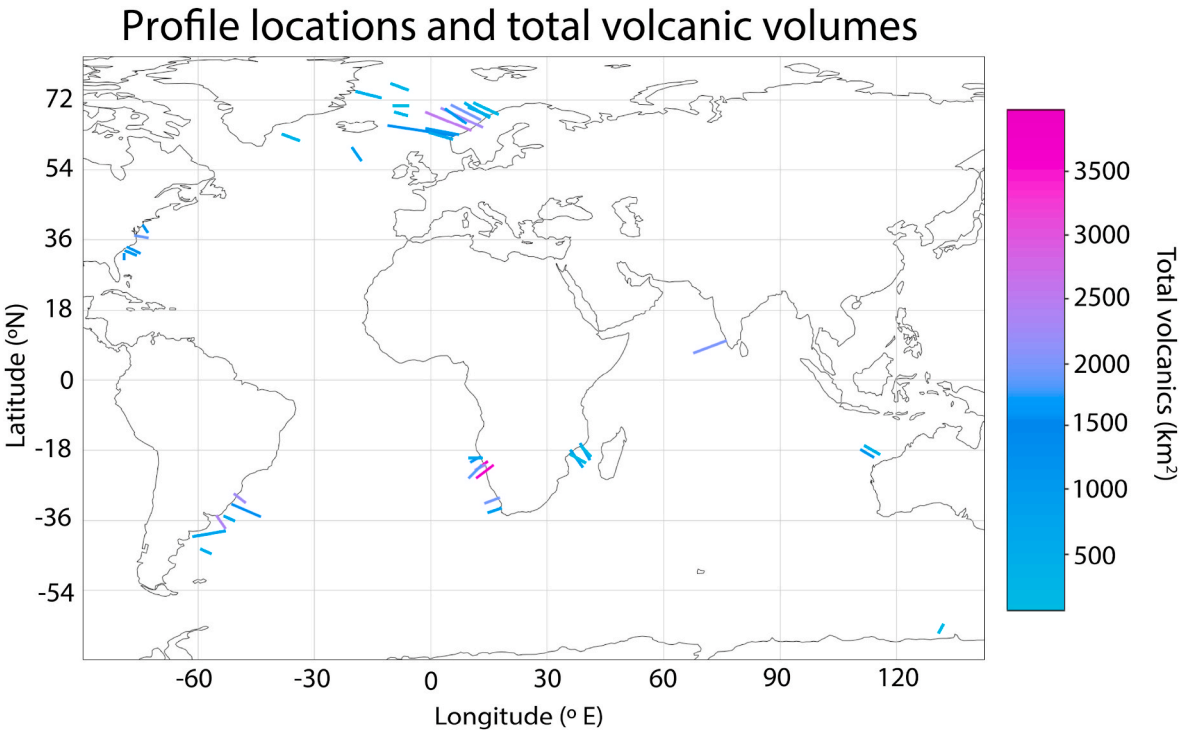

Fig. 4. Locations of previously published seismic profiles included in VOLMIR with line colors correlating to the volume of total volcanics.

ratio of 1.95, is the Gernigon West line near Greenland (Gernigon et al., 2015). This location is interpreted as a remnant of the continental marginal plateau and thus does not contain the full passive margin (Gernigon et al., 2015). It is likely that this area was separated from the rest of the margin, and some of the associated HVLC did not remain attached to the portion of crust containing the SDR.

The relatively consistent average ratio suggests that formation of the SDR and HVLC units are genetically related during continental rifting and breakup, as discussed later. Presumably, as a lower density melt rises to form SDRs, the remaining high-density residuum or cumulate becomes the HVLC. Mantle-melt interaction and magma processing at the crust/mantle boundary over an extended period would produce a pyroxenitic cumulate mush from which melt is extracted (e.g. Rooney et al., 2017). This melt would then erupt as moderately evolved basalts to form SDRs. This process would be analogous to that proposed based on data from present and past areas of continental rifting (Vervoort et al., 2007; Thybo and Artemieva, 2013).

4.3. Distances from Euler pole and hotspot associated with rifting

For margins in the Atlantic Ocean, we compiled the associated Euler pole and hotspot locations at the time of continental breakup/margin formation. The profiles were split into groups, representing the North Atlantic, Mid-Atlantic, and South Atlantic. Each group's associated Euler pole, hotspot, and time of breakup are listed in Table 3.

SDR volumes versus the angular distance of each margin from the associated Euler pole and hotspot at the time of continental breakup are shown in Fig. 6. Due to the previously mentioned difficulty in resolving HVLC units, and that HVLC can develop over multiple cycles (e.g. Rooney et al., 2017), we consider SDR volumes to be the most robust volcanic unit for comparison. As mentioned, the observed relatively consistent ratios between SDR and HVLC volumes indicate that SDR volumes are proportional to overall total volcanic volumes. The location of the margin determined through past reconstructions via GPlates (Table 4) represents a midpoint along the seismic line.

The volumes of igneous rocks on different profiles are moderately positively correlated with distances from the Euler pole (Fig. 7). In contrast, the volumes show a weak negative correlation with distance from the nearest hotspot. These trends are expected, because more magma should be generated at locations further from the Euler pole, where spreading rates are faster and thus net extension greater, and more melt should be generated closer to a hotspot. The relative strengths of the correlations suggest that in continental breakup lithospheric processes, which are termed passive rifting, as discussed shortly, have greater effects than hotspots, termed active rifting. This view is consistent with studies (Lundin et al., 2014, 2018) that find a correlation between extension rates and magma production during rifting.

5. Potential applications of the dataset we have compiled and present

We envision the VOLMIR dataset being valuable for various studies addressing fundamental questions about rifting, breakup, and passive margin formation that remain unresolved despite extensive studies and proposed alternative models. These include:

5.1. How do continental rifting and breakup generate such large volumes of magmatic rocks?

Despite its importance, much remains to be learned about how and why continental rifting occurs. Two end-member models (Fig. 8) have been discussed for many years (Sengor and Burke, 1978). In one, "active" rifting and breakup are a response to melting in the underlying asthenosphere or deeper mantle as a result of mantle plumes or shallower thermal or compositional anomalies, as commonly proposed for the East African Rift (Ebinger and Sleep, 1998). In the other, continental rifting and breakup are a "passive" response to stresses transmitted within the lithosphere, as appears to be the case along the Baikal Rift where the Amurian plate diverges from Eurasia (Calais et al., 2003).

It is consequently unclear whether large-scale magmatism is a cause or effect of rifting, and the associated mantle dynamics remain unresolved. A key aspect of this issue is how the large volumes of igneous rocks at passive margins are generated. It has long been proposed that excess temperatures associated with hotspots/plumes are required to rift

Table 1
Profiles included in VOLMIR with their original publication, figure number from the original publication, unit names from the original publication, and which criteria each unit satisfied for our reinterpretation.

Profile	Original Publication	Figure	Name of SDR unit	Reclassification criteria satisfied for SDR	Name of HVLC unit	Reclassification criteria satisfied for HVLC
Pelotas	Blaich et al. (2011)	9	Pre/syn rift, SDRs	1, 3, 4	Transitional domain	1, 2, 3, 4
Walvis	Blaich et al. (2011)	10	Pre/syn rift, SDRs	1, 3, 4	Transitional domain	1, 2, 3, 4
Colorado	Blaich et al. (2011)	12	Pre/syn rift, SDRs	1, 3, 4	Transitional domain	1, 2, 3, 4
Orange	Blaich et al. (2011)	12	Pre/syn rift, SDRs	1, 3, 4	Transitional domain	1, 2, 3, 4
Lofoten-Vesterålen	Faleide et al. (2008)	3	Extrusives	1, 3	7+ km/s lower crustal body	1, 3
Lofoten	Faleide et al. (2008)	3	Extrusives	1, 3	7+ km/s lower crustal body	1, 3
Vøring4	Faleide et al. (2008)	3	Extrusives	1, 3	7+ km/s lower crustal body	1, 3
Vøring3	Faleide et al. (2008)	3	Extrusives	1, 3	7+ km/s lower crustal body	1, 3
Vøring2	Faleide et al. (2008)	3	Extrusives	1, 3	7+ km/s lower crustal body	1, 3
Møre	Faleide et al. (2008)	3	Extrusives	1, 3	7+ km/s lower crustal body	1, 3
801 Mid Atlantic	Holbrook and Talwani (1994)	15	Basalt (just left edge)	1, 3, 5	high-MgO Intrusives, mafic intrusives	1, 2, 3, 4
Uruguay	Becker et al. (2014)	5	SDR's	1	HVLC	1, 3
Transect 4 Namibia	Gladczenko et al. (1998)	14	SDR's	1, 3	LCB, Transitional crust	1, 2, 3, 4
Gernigon East	Gernigon et al. (2015)	13	SDRs	1	LCB	1, 2
GernigonWest	Gernigon et al. (2015)	13	SDRs, landward lava flows	1	LCB	1, 2
Eldholm and Grue A	Eldholm and Grue (1994)	2	Flood basalts	1, 3	High velocity lower crust	1, 2
Eldholm and Grue A′	Eldholm and Grue (1994)	2	Flood basalts	1, 3	High velocity lower crust	1, 2
Eldholm and Grue B	Eldholm and Grue (1994)	2	Flood basalts	1, 3	High velocity lower crust	1, 2
Eldholm and Grue B′	Eldholm and Grue (1994)	2	Flood basalts	1, 3	High velocity lower crust	1, 2
Eldholm and Grue C	Eldholm and Grue (1994)	3	Flood basalts	1, 3	High velocity lower crust	1, 2
Eldholm and Grue C′	Eldholm and Grue (1994)	3	Flood basalts	1, 3	High velocity lower crust	1, 2
Eldholm and Grue D	Eldholm and Grue (1994)	3	Flood basalts	1, 3	High velocity lower crust	1, 2
Eldholm and Grue D′	Eldholm and Grue (1994)	3	Flood basalts	1, 3	High velocity lower crust	1, 2
LASE	Biari et al. (2017)	4	Seaward dipping reflectors	1, 3	Underplated region	1, 2, 3
USGS-32	Biari et al. (2017)	4	Seaward dipping reflectors	1, 3	Underplated region	1, 2, 3
Ba-6	Biari et al. (2017)	4	Seaward dipping reflectors	1, 3	Underplated region	1, 2, 3
BGR98-20	Franke (2013)	14	SDRs	1	High velocity lower crust	1
BGR03-16a	Franke (2013)	14	SDRs	1	High velocity lower crust	1
Transect 3 Namibia	Gladczenko et al. (1998)	5	SDRs/Breakup related extrusive complexes	1, 3, 4	LCB	1, 3
Transect 2 Namibia	Gladczenko et al. (1998)	4	SDRs/Breakup related extrusive complexes	1, 3, 4	LCB	1, 3
Punta del Este	Reuber and Mann (2019)	3	SDR/Igneous crust	1, 3	NA	
Pelotas South	Reuber and Mann (2019)	4	SDR/Igneous crust	1, 3	NA	
Luderitz	Reuber and Mann (2019)	4	SDR/Igneous crust	1, 3	NA	
Carolina Trough	Tréhu et al. (1989)	13	Seaward dipping reflections	1	High velocity lower crust	1
Transect 1	Fernàndez et al. (2010)	3	SDRs	1	High velocity zone 1/2/ Underplating	1, 3
AWI-20070201	Mueller and Jokat (2017)	8	SDRs, intrusions	1	HVLCB	1, 3, 4
AWI-20140010	Mueller and Jokat (2017)	8	Lava flows	1, 3	HVLCB	1, 3, 4
Senkans Profile A	Senkans et al., 2019	3	SDR	1	NA	
Senkans Profile C	Senkans et al. (2019)	7	SDR	1	NA	
USGS line 3	Eittriem (1994)	11	V2 - Seaward dipping reflectors	1	NA	
110/15	Frey et al., 1998	4	SDR	1	Lower crust	1, 3
128/08	Frey et al., 1998	4	SDR	1	Lower crust	1, 3
RE23	Ajay et al. (2010)	5	SDR	1	LCB	2, 3

Table 2
Volcanic unit volumes for profiles in VOLMIR. While these measurements are cross sectional areas of the units, we assume that the cross-sectional area is proportional to the volume in the adjacent region.

Profile	Total SDR area (km^2)	HVLC area (km^2)	Total Volcanic (km^2)
Pelotas	651	1566	2217
Walvis	1100	2892	3992
Colorado	287	521	808
Orange	556	1361	1916
Lofoten-Vesterålen	82	145	227
Lofoten	141	472	612
Vøring4	250	1667	1916
Vøring3	221	2027	2248
Vøring2	410	2102	2513
Møre	145	1241	1386
801 Mid Atlantic	559	1308	1867
Uruguay	167	563	730
Transect 4 Namibia	389	1899	2288
Gernigon East	185	459	644
GernigonWest	175	90	266
Eldholm and Grue A	106	341	447
Eldholm and Grue A′	97	155	252
Eldholm and Grue B	195	926	1121
Eldholm and Grue B′	173	266	439
Eldholm and Grue C	234	884	1118
Eldholm and Grue C′	44	0	44
Eldholm and Grue D	253	724	976
Eldholm and Grue D′	341	0	341
LASE	216	1077	1293
USGS-32	197	1099	1297
Ba-6	148	1026	1174
BGR98-20	210	335	545
BGR03-16a	367	642	1009
Transect 3 Namibia	949	612	1561
Transect 2 Namibia	165	570	736
Punta del Este	2356	0	2356
Pelotas South	1526	0	1526
Luderitz	1808	0	1808
Carolina Trough	85	1178	1262
Transect 1	321	3391	3712
AWI-20070201	81	796	878
AWI-20140010	51	743	794
Senkans Profile A	184	0	184
Senkans Profile C	136	0	136
USGS line 3	139	0	139
110/15	203	970	1173
128/08	66	327	393
RE23	34	1935	1969
Mean	**372**	**844**	**1217**
Median	**197**	**642**	**1118**
Standard deviation	**485**	**803**	**914**

continents apart, given the large volumes of igneous rocks at most passive margins (Burke and Whiteman, 1973; Morgan, 1981, 1983; White and McKenzie, 1989; Richards et al., 1989; Armitage and Collier, 2017). However, invoking plumes for all LIPs and rifted margins has been questioned (Kelemen and Holbrook, 1995) and alternatives have been proposed (King and Anderson, 1995; McHone, 2000; King, 2007; Foulger, 2011). van Wijk et al. (2001, 2004) favor generation of volcanic margins by decompression melting alone without the aid of mantle plumes. Franke (2013) finds that the rifting and spreading history of the South Atlantic, a classic volcanic margin, cannot be reconciled with a mantle plume model. How long linear rifts can be generated from a plume remains unclear and under investigation (Koptev et al., 2017; Beniest et al., 2017). The volume of magmatic rocks is a crucial

Table 4
Locations of the midpoint of each profile and its angular distance from Euler pole and hotspot, at the time of formation. Atlantic margins only.

Profile	Latitude (at formation) (°)	Longitude (at formation) (°)	Angular distance from hotspot (°)	Angular distance from pole (°)	North, Mid or South Atlantic
Pelotas	−28.56	−46.49	8.20	80.29	S
Walvis	−29.43	−43.98	6.76	80.84	S
Colorado	−37.77	−52.43	7.97	90.26	S
Orange	−38.13	−47.94	4.67	89.93	S
Lofoten-Vesterålen	67.45	1.85	11.15	46.50	N
Lofoten	66.42	0.52	10.89	47.65	N
Vøring4	66.23	−3.30	9.48	48.35	N
Vøring3	65.10	−4.48	9.40	49.58	N
Vøring2	63.90	−8.08	8.55	51.17	N
Møre	62.29	−13.78	7.50	53.36	N
801 Mid Atlantic	20.95	−45.45	4.96	50.64	M
Uruguay	−33.82	−49.04	5.70	85.85	S
Transect 4 Namibia	−29.72	−44.37	6.54	81.17	S
Gernigon East	60.45	−5.09	11.76	54.10	N
GernigonWest	66.28	−13.56	5.48	49.44	N
Eldholm and Grue A	67.21	0.71	10.71	46.88	N
Eldholm and Grue A′	68.31	−1.78	9.67	46.20	N
Eldholm and Grue B	61.54	−3.76	11.52	52.87	N
Eldholm and Grue B′	65.97	−7.51	7.92	49.12	N
Eldholm and Grue C	61.56	−8.61	9.76	53.50	N
Eldholm and Grue C′	66.25	−9.40	7.11	49.06	N
Eldholm and Grue D	57.23	−28.44	9.91	59.38	N
Eldholm and Grue D′	57.79	−30.08	9.43	58.87	N
LASE	23.32	−44.53	2.91	48.13	M
USGS-32	18.29	−47.44	7.70	53.72	M
Ba-6	17.53	−47.94	8.53	54.58	M
BGR98-20	−40.31	−54.13	9.93	93.04	S
BGR03-16a	−40.69	−49.51	7.05	92.67	S
Transect 3 Namibia	−27.45	−44.88	8.85	78.99	S
Transect 2 Namibia	−27.24	−44.87	9.05	78.78	S
Punta del Este	−34.95	−50.81	6.72	87.23	S
Pelotas South	−30.78	−47.50	6.67	82.63	S
Luderitz	−30.86	−44.79	5.53	82.35	S
Carolina Trough	17.71	−47.70	8.31	54.35	M
Transect 1	−29.79	−44.51	6.50	81.29	S

Table 3
Time of breakup, Euler pole, and hotspot locations (at margin formation) for North, Mid, and South Atlantic margins.

Part of Atlantic	Time of Breakup (Ma)	Associated hotspot	Hotspot latitude (at breakup) (°)	Hotspot longitude (at breakup) (°)	Euler pole latitude (at breakup) (°)	Euler pole longitude (at breakup) (°)
North	55	Iceland	67.13	−27.29	63.25	144.00
Mid	175	Canary Island	25.88	−46.05	66.95	−12.02
South	125	Tristan de Cunha	−36.10	−42.67	50.76	−32.39

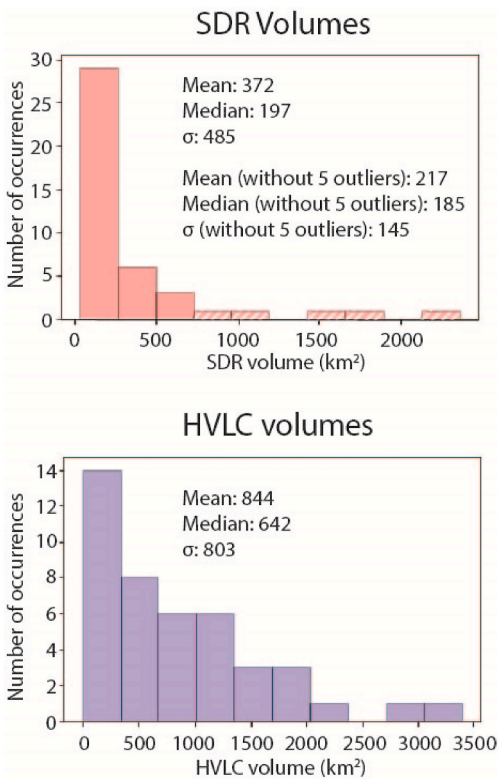

Fig. 5. SDR and HVLC volumes with mean, median, and standard deviation. SDR plot also includes mean, median, and standard deviation when five outliers (dashed pattern; > 900 km^2) are excluded from the dataset.

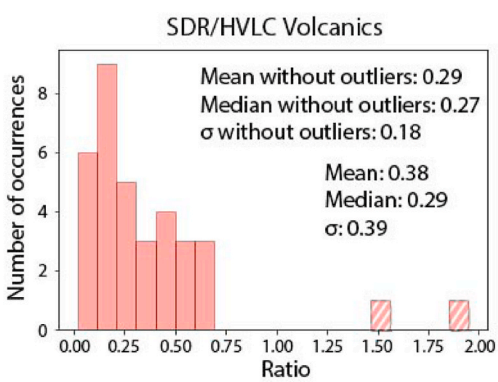

Fig. 6. Ratio of SDR/HVLC material. Plot excludes margins where no HVLC could be resolved. Outliers (dashed pattern) around 1.50 and 1.90 are likely due to poorly resolved imaging at depth or other complex breakup patterns discussed in the text.

constraint that can be used in numerical modeling of their formation (e.g., Kelemen and Holbrook, 1995; White et al., 2008; Gunawardana et al., 2019).

Our initial results show that igneous rock volumes are weakly negatively correlated with distance from the nearest hotspot. The stronger correlation with distance from the Euler pole suggests that in continental breakup, lithospheric processes (passive rifting) have greater effects than hotspots (active rifting), as discussed shortly. Further analysis of these data is likely to yield additional insights.

It is worth noting that our volumes reflect only volcanism associated with the rifted margin, and do not include on-land volcanism, seafloor volcanism in the hotspot track (e.g., Walvis Rise), or seamounts. These would need to be included in modeling the effects of a hotspot.

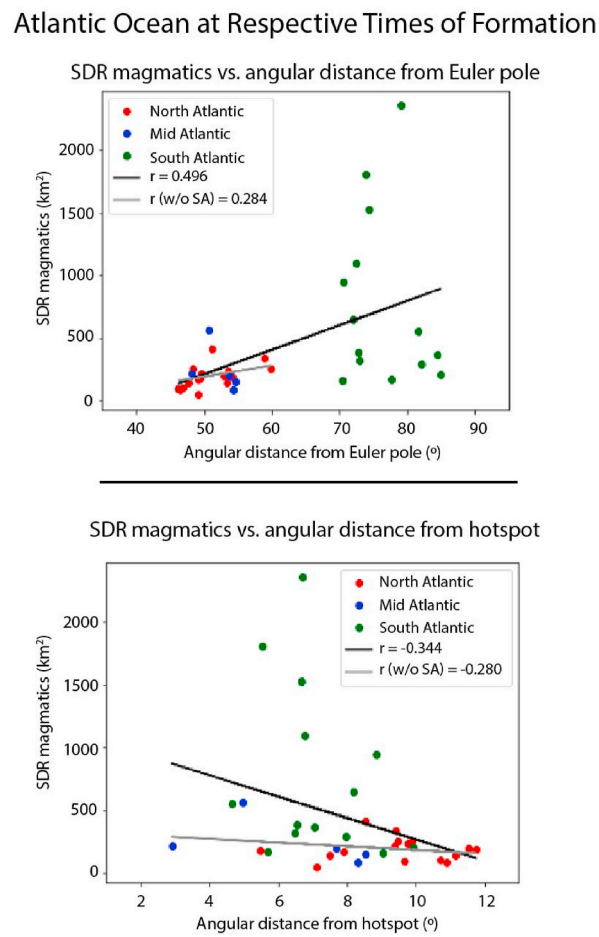

Fig. 7. (Top) SDR volcanic volumes vs. distance from the Euler pole and (bottom) hotspot at the time of margin formation. These only include margins from the Atlantic Ocean. Gray lines (labeled w/o SA) show correlations without the South Atlantic data, which are weaker.

5.2. How are the SDR and HVLC units related?

HVLC are examples of underplating, defined as an "addition of mafic magma to the lower crust and uppermost mantle around the Moho" (Thybo and Artemieva, 2013). Underplating, indicated by high-velocity bodies, is also often observed in continental rifts (e.g., Maguire et al., 2006; Rooney et al., 2017), and has been attributed to a wide variety of processes. Often, the HVLC bodies are interpreted as formed from residual melt after extraction of low-density SDR lavas, analogous to the high-density residual melt cumulate underplated layers ponded at the base of the crust in areas of continental rifting and breakup (Fig. 9) (e.g., Vervoort et al., 2007; Thybo and Artemieva, 2013). This view is supported by the fact that SDRs usually overlie HVLC units. However, Becker et al. (2014) note that in parts of the South Atlantic margin, HVLC extend "far seaward" of the SDRs, and suggest that these SDRs and HVLCs formed at different times during rifting and breakup. In another alternative model, White et al. (2008) interpret HVLCs as resulting from sills intruded into the lower crust.

SDRs and HVLC are units characterized primarily by seismic imaging that have identified dense regions interpreted as igneous material. SDRs or HVLC are rarely sampled in order to more fully constrain their origin. This creates ambiguities as to the precise petrogenesis of these units.

As discussed earlier, SDRs are considered basaltic flows associated with continental breakup. Basalts erupted in both oceanic ridges and continental rifts are not primary and require differentiation (typically by fractional crystallization) prior to eruption. In oceanic crust, such

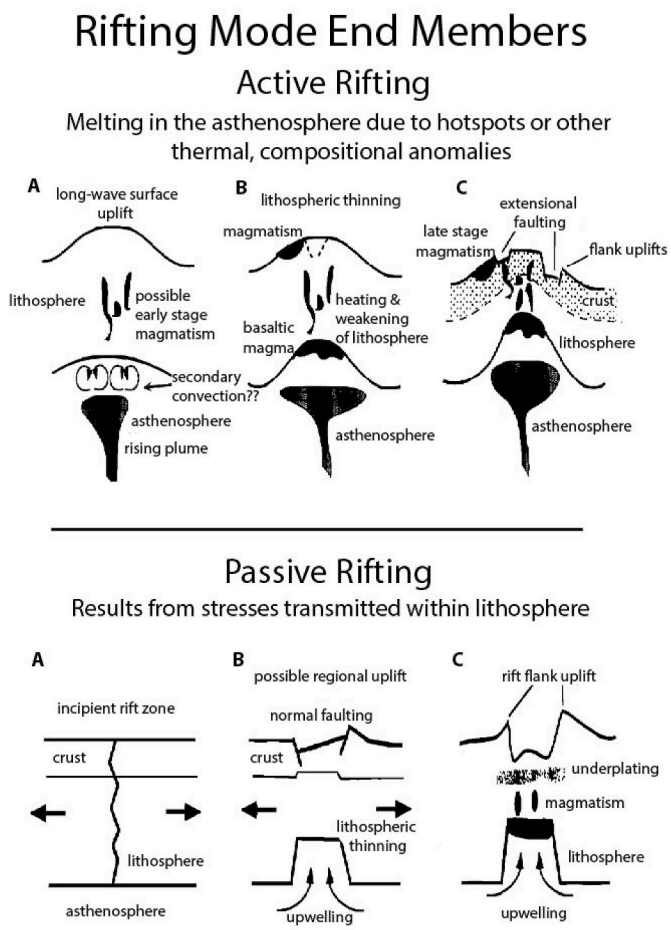

Fig. 8. Schematic illustration of end member rifting models (Ruppel, 1995).

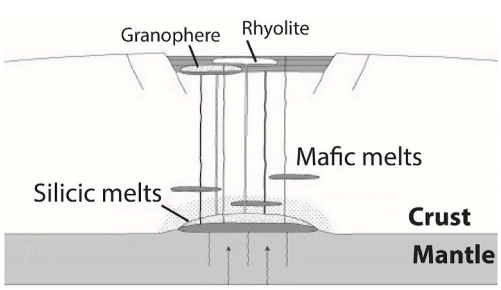

Fig. 9. Model for Midcontinent Rift magmatism showing formation of an underplated layer analogous to the HVLC layer at passive margins (Vervoort et al., 2007).

differentiation is thought to occur within crystal-magma mush zones within the lower crust. In continental environments, such mush zones can be distributed throughout the crust. The transitional region between continental rifting and oceanic spreading where SDRs are focused thus likely exhibits characteristics of transitional magmatic plumbing systems. Although the precise locations of such mush zones remain unclear in such transitional regions, the processes operating within them are likely similar, at least at lower crustal levels.

In the most basic sense, basalts undergo differentiation somewhere within the thinned crust, leaving behind a mass of crystal cumulate that would, upon solidification, appear denser than the surrounding continental crust. Such mush zones may be active over an extended interval (forming 'hot zones') (Cashman et al., 2017) wherein many generations of crystals may accumulate. Such regions may represent the HVLC imaged by seismic techniques. Alternatively, if a sufficient volume of basaltic magma was intruded as sills into the lower crust (White et al., 2008), such cooled intrusions could also result in HVLC. In all likelihood there are multiple mechanisms by which HVLC is generated.

Where samples of HVLC have been retrieved in xenolith suites from Ethiopia, it is apparent that multiple generations of pyroxene-rich cumulates comprise these intrusions (Rooney et al., 2017). However, the antiquity of these cumulates is nevertheless unknown – they may represent cumulate material that spans events that date back to the formation of this crust during the Pan-African orogeny, Oligocene flood basalts differentiation, to more modern lavas associated with rifting. The varied mechanisms and times at which HVLC may develop could thus result in a disconnect between the thickness of an SDR package and the size of the associated HVLC.

5.3. What causes variability in structure along margins and between conjugate margins?

Asymmetric features are often observed on opposite sides of conjugate margins, where the SDR zone is wider on one side than the other (e.g., Blaich et al., 2011; Reuber et al., 2019). In some places, the width of the SDR zone also varies along the margin (McDermott et al., 2018). How these variations arise is unclear: Becker et al. (2014) find that the HVLC units on the South African margin are much wider than on the South American side, in contrast to the pattern of the continental flood basalts. Asymmetries have been attributed to effects including hotspot geometry (Reuber et al., 2019), rifting geometry (Becker et al., 2014), and variations in lithospheric strength and extension rates (Svartman Dias et al., 2015).

5.4. Are volcanic volume and geometry variations associated with microcontinents and other details of the rifting and early spreading processes?

Continental rifting and early seafloor spreading often involve geometric complexities, such as propagating rifts and microplates, as observed along the East African Rift (Saria et al., 2013) and recorded in the marine magnetic record (e.g., Acton et al., 1991; Franke, 2013; Greene et al., 2017). In particular, rifting sometimes leaves isolated pieces of continental crust surrounded by oceanic crust, outboard of passive margins, such as the Jan Mayen microcontinent (Gaina et al., 2009; Schiffer et al., 2018). Various models for how this occurs have been offered. Müller et al. (2001) propose that along the landward edge of a rifted margin, the margin's weakness may be enhanced by heating from a mantle plume, causing a spreading ridge to propagate into this weak zone. Molnar et al. (2018) propose that microcontinent formation may be restricted to localized regions along passive margins associated with preexisting zones of lithospheric weakness.

5.5. How do the volumes and geometries of igneous rocks at magma-rich margins compare to those in presently active and failed continental rifts and continental LIPs?

The rifting process that forms passive margins also forms large igneous provinces on land, such as the Central Atlantic Magmatic Province, or CAMP (Marzoli et al., 1999; McHone, 2000, 2020; Hames et al., 2002) associated with the Mid-Atlantic rifted margins included in the VOLMIR dataset.

Some insight into these issues can be obtained by considering failed rifts. Because the architecture of the margin is the final result of continental breakup, the volume and geometry of the volcanic units at failed rifts preserve aspects of rifting that are altered or hard to see at successful rifts, and thus can give insight into the rifting process. For example, we have been considering similarities between volcanic passive margins and North America's 1.1 Ga Midcontinent Rift (MCR) that formed as part of the rifting of Amazonia from Laurentia (Stein et al.,

2015, 2018a, 2018b). Although the MCR is not fully representative of all volcanic margin formation processes, if only because it failed to evolve to seafloor spreading, it has many similarities to volcanic margins.

Surface exposures, seismic, and gravity data delineate a rift basin filled by inward dipping flood basalt layers, underlain by thinned and underplated crust, recording a history of extension, volcanism, sedimentation, subsidence, and inversion (Fig. 10). The overall structure is similar to that of a rifted margin, with the dipping flows analogous to SDRs at a rifted margin, and the underplate analogous to the HVLC at rifted margins. The basin-filling volcanics give rise to prominent magnetic anomalies, analogous to the large magnetic anomalies at rifted margins that occur landward of the oldest spreading anomalies. Interestingly, the ratio of the cross-sectional area of rift-filling volcanics to that of underplated material at the MCR is much higher, about 1.0–1.5, than at rifted margins (which we found to be ~0.3–0.4, as discussed) (Elling et al., 2020), presumably because the MCR did not evolve to seafloor spreading.

On the profile shown (Fig. 10), the Douglas/Ojibwa Fault on the north side of the basin was the master fault active during rifting, so it truncates the layered flows. In contrast, the Keweenaw Fault on the south side is subparallel to the base of the volcanic infill, indicating it was not a major rift-bounding normal fault during the extension. Conversely, the Keweenaw fault was the master fault on a seismic line to the east. This polarity reversal along a series of adjacent half-graben segments (Dickas and Mudrey, 1997) is analogous to that in the East African rift (Ebinger, 2012; Heilman et al., 2019). These structures are easily observed because of the combination of high-quality seismic data across Lake Superior and the fact that the structure was later inverted by regional compression resulting in 10–15 km of uplift and erosion exposing the volcanic rocks.

The MCR gives a snapshot of deposition of a thick, dense, and highly magnetized volcanic section during rifting. It came close to evolving into an oceanic spreading center, but failed and so records a late stage of rifting. It thus gives insight into how rifting and volcanism interacted in the early phase of volcanic margin formation, a record that is lost and not observable at the surface if a rift evolves to seafloor spreading. It is useful to view the MCR as a preserved piece of what might have evolved to a volcanic margin had the MCR not failed. In that case, extension would have continued so the thick post-rift volcanics and sediments would not have been deposited in a narrow subsiding sag basin. Instead they would have been deposited over a larger area as extension continued, splitting the continent, and evolving into seafloor spreading. Many of the main features seen at magma-rich passive margins could have formed this way, though they would be modified. As extension continued, the flows that dip toward the rift basin center would give rise to packages of SDRs, whose final geometry could also reflect additional normal faulting, flexure, or other effects (Buck, 2017; Morgan and Watts, 2018; Tian and Buck, 2019). Additional SDRs could be deposited as seafloor spreading starts (Koopmann et al., 2014).

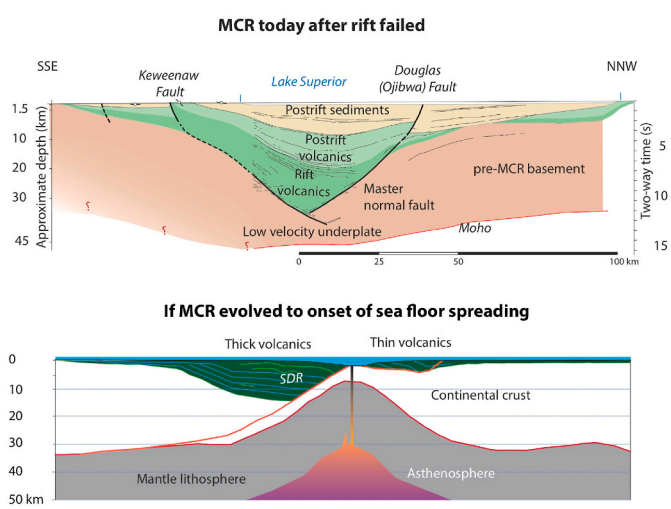

Fig. 10. Top: Present Midcontinent Rift structure, generalized by combining seismic profiles across Lake Superior with land geology. Bottom: A scenario by which the MCR could have yielded an asymmetric passive margin after continued half-graben rifting. Post-rift volcanics and sediments would not have been deposited in a narrow subsiding basin. Instead, they would have been deposited over a larger area as extension continued, splitting the continent, and evolving into seafloor spreading (Stein et al, 2018a). If the basin split along the master fault, both sides could have similar amounts of the HVLC underplate, but differences in the volume of flows (i.e. SDRs).

The MCR analogy also suggests a mechanism for passive margin symmetry or asymmetry. If the basin split at its deepest point, symmetric passive margins would result. If the basin split elsewhere, perhaps along the master fault as illustrated in Fig. 10 (bottom), it would have yielded asymmetric margins, like those observed in some areas. In this case, both sides could have similar amounts of the HVLC underplate (depending on whether and how the faulting extended to the lower crust), but differences in the volume of flows (i.e. SDRs). The asymmetry would result not from asymmetric volcanism, but from the way the flows were rifted apart. Thus, igneous rock volumes may distinguish between asymmetry due to hotspot geometry, which would affect SDRs and HVLC similarly, and asymmetry due to rifting geometry, which could affect the two differently.

5.6. Do rifted margin structure and evolution influence which margins have large earthquakes?

Eastern North America's passive continental margin, like others, is "passive-aggressive" with a moderate level of seismicity (Stein et al., 1979, 1989; Schulte and Mooney, 2005; Wolin et al., 2012; Neely et al., 2018). Some passive margins have larger earthquakes than others, for reasons that are unclear. Why this difference arises is both scientifically interesting and important for assessing earthquake, tsunami (Ten Brink et al., 2014), and landslide (Hill et al., 2018) hazards.

6. Conclusions

Rifted continental margins are a major research area for their scientific significance and their importance for both energy resources and natural hazards - landslides, tsunamis, and earthquakes. Further studies into these margins could drive developments in our understanding of how and why continents rift, as well as why these rifts sometimes fail. The VOLMIR dataset provides useful insights into some of these processes through analysis of the amount of volcanic material present along rifted margins. The key patterns observed are:

1) A relatively consistent ratio of SDR to HVLC volumes, where SDR amounts are approximately 1/3 of that of HVLC. This ratio suggests that the units are related during formation. Further analysis of these ratios could provide insight into how these units form during the continental rifting/breakup process.
2) The volumes of SDR units are moderately positively correlated with distance from the Euler pole, and weakly negatively correlated with distance from the nearest hotspot. These trends are consistent with present understanding of each of these factors (magma volume is greater further from the Euler pole where spreading is fastest, and closer to a hotspot where the largest melting occurs). The relative strength of the correlations suggests that lithospheric processes play more of a role in continental rifting and breakup than hotspot/mantle plume processes.

Declaration of competing interest

The authors declare that they have no known competing financial interests or personal relationships that could have appeared to influence

the work reported in this paper.

Acknowledgements

We thank Tiago Alves and an anonymous reviewer for helpful reviews and Daniel Brennan for useful comments. This research was supported by NSF grants EAR-0952345 and EAR-1549920.

References

Acton, G.D., Stein, S., Engeln, J.F., 1991. Block rotation and continental extension in Afar: a comparison to oceanic microplate systems. Tectonics 10 (3), 501–526.
Ajay, K.K., Chaubey, A.K., Krishna, K.S., Gopala Rao, D., Sar, D., 2010. Seaward dipping reflectors along the SW continental margin of India: evidence for volcanic passive margin. Journal of Earth System Science 119 (6), 803–813.
Alves, T., Cunha, T.A., 2018. A phase of transient subsidence, sediment bypass and deposition of regressive-transgressive cycles during the breakup of Iberia and Newfoundland. Earth Planet Sci. Lett. 484, 168–183.
Alves, T., Fetter, M., Busby, C., Gontijo, R., Cunha, T.A., Mattos, N.H., 2020. A tectono-stratigraphic review of continental breakup on intraplate continental margins and its impact on result hydrocarbon systems. Mar. Petrol. Geol. 117.
Armitage, J.J., Collier, J.S., 2017. The thermal structure of volcanic passive margins. Petrol. Geosci. 24, 393–401.
Austin Jr., J.A., Stoffa, P.L., Phillips, J.D., Oh, J., Sawyer, D.S., Purdy, G.M., Reiter, E., Makris, J., 1990. Crustal structure of the Southeast Georgia embayment-Carolina trough: preliminary results of a composite seismic image of a continental suture (?) and a volcanic passive margin. Geology 18 (10), 1023–1027.
Becker, K., Franke, D., Trumbull, R., Schnabel, M., Heyde, I., Schreckenberger, B., Koopmann, H., Bauer, K., Jokat, W., Krawczyk, C.M., 2014. Asymmetry of high-velocity lower crust on the South Atlantic rifted margins and implications for the interplay of magmatism and tectonics in continental breakup. Solid Earth 5 (2), 1011–1026.
Beniest, A., Koptev, A., Leroy, S., Sassi, W., Guichet, X., 2017. Two-branch break-up systems by a single mantle plume: insights from numerical modeling. Geophys. Res. Lett. 44 (19), 9589–9597.
Biari, Y., Klingelhoefer, F., Sahabi, M., Funck, T., Benabdellouahed, M., Schnabel, M., Reichert, C., Gutscher, M.A., Bronner, A., Austin, J.A., 2017. Opening of the central Atlantic Ocean: implications for geometric rifting and asymmetric initial seafloor spreading after continental breakup. Tectonics 36 (6), 1129–1150.
Blaich, O.A., Faleide, J.I., Tsikalas, F., 2011. Crustal breakup and continent-ocean transition at South Atlantic conjugate margins. J. Geophys. Res.: Solid Earth 116 (B1).
Bronner, A., Sauter, D., Manatschal, G., Péron-Pinvidic, G., Munschy, M., 2011. Magmatic breakup as an explanation for magnetic anomalies at magma-poor rifted margins. Nat. Geosci. 4 (8), 549–553.
Buck, W.R., 2017. The role of magmatic loads and rift jumps in generating seaward dipping reflectors on volcanic rifted margins. Earth Planet Sci. Lett. 466, 62–69.
Burke, K., Whiteman, A.J., 1973. Uplift, rifting and the break-up of Africa. Implications of continental drift to the Earth Sciences 2 (part 7), 735–755.
Busby, C., Azor Pérez, A., 2012. Tectonics of Sedimentary Basins: Recent Advances. Wiley -Blackwell, p. 664.
Calais, E., Vergnolle, M., San'Kov, V., Lukhnev, A., Miroshnitchenko, A., Amarjargal, S., Déverchère, J., 2003. GPS measurements of crustal deformation in the Baikal-Mongolia area (1994–2002): implications for current kinematics of Asia. J. Geophys. Res.: Solid Earth 108 (B10).
Cashman, K.V., Sparks, R.S.J., Blundy, J.D., 2017. Vertically extensive and unstable magma systems: a unified view of igneous processes. Science 355 (6331).
Davis, J.K., Becel, A., Shillington, D.J., Buck, W.R., 2018. The distribution and characteristics of seaward dipping reflectors along the eastern North American Margin. AGU Fall Meeting Abstracts.
Dewey, J.F., Burke, K., 1974. Hot spots and continental break-up: implications for collisional orogeny. Geology 2 (2), 57–60.
Dickas, A.B., Mudrey, M.G., 1997. Segmented structure of the middle Proterozoic Midcontinent Rift system, North America. In: Ojakangas, R.W., Dickas, A.B., Green, J.C. (Eds.), Middle Proterozoic to Cambrian Rifting, Central North America. Geological Society of America Special Paper 312, Boulder, Colorado, pp. 37–46.
Diebold, J.B., Stoffa, P.L., LASE Study Group, 1988. A large aperture seismic experiment in the Baltimore Canyon Trough. In: Sheridan, R., Grow, J.A. (Eds.), The Geology of North America, I-2. *The Atlantic Continental Margin, US*, pp. 387–398.
Ebinger, C., 2012. Evolution of the Cenozoic East African rift system: cratons, plumes and continental breakup. In: Regional Geology and Tectonics: Phanerozoic Rift Systems and Sedimentary Basins, vol. 1. Elsevier, Boston, pp. 132–162.
Ebinger, C.J., Sleep, N.H., 1998. Cenozoic magmatism throughout east Africa resulting from impact of a single plume. Nature 395 (6704), 788–791.
Eddy, D.R., Van Avendonk, H.J.A., Christeson, G.L., Norton, I.O., Karner, G.D., Johnson, C.A., Snedden, J.W., 2014. Deep crustal structure of the northeastern Gulf of Mexico: implications for rift evolution and seafloor spreading. J. Geophys. Res.: Solid Earth 119, 6802–6822.
Eittriem, S.L., 1994. Transition from continental to oceanic crust on the Wilkes-Adelie margin of Antarctica. J. Geophys. Res. 99 (B12), 24189–24205.
Eldholm, O., Grue, K., 1994. North Atlantic volcanic margins: dimensions and production rates. J. Geophys. Res.: Solid Earth 99 (B2), 2955–2968.
Elling, R.P., Stein, S., Stein, C.A., Keller, G.R., 2020. Tectonic implications of the gravity signatures of the Midcontinent Rift and Grenville Front. Tectonophysics 778, 228369.
Faleide, J.I., Tsikalas, F., Breivik, A.J., Mjelde, R., Ritzmann, O., Engen, O., Wilson, J., Eldholm, O., 2008. Structure and evolution of the continental margin off Norway and the Barents Sea. Episodes 31 (1), 82–91.
Fernàndez, M., Afonso, J.C., Ranalli, G., 2010. The deep lithospheric structure of the Namibian volcanic margin. Tectonophysics 481, 68–81.
Foulger, G.R., 2011. Plates vs Plumes: a Geological Controversy. John Wiley & Sons.
Foulger, G.R., Jurdy, D.M. (Eds.), 2007. Plates, Plumes and Planetary Processes. Geological Society of America Special Paper, p. 430.
Franke, D., 2013. Rifting, lithosphere breakup and volcanism: comparison of magma-poor and volcanic rifted margins. Mar. Petrol. Geol. 43, 63–87.
Frey, Ø., Planke, S., Symonds, P.A., Heeremans, M., 1998. Deep crustal structure and rheology of the Gascoyne volcanic margin, western Australia. Mar. Geophys. Res. 20 (4), 293–311.
Gaina, C., Gernigon, L., Ball, P., 2009. Palaeocene–recent plate boundaries in the NE Atlantic and the formation of the Jan Mayen microcontinent. J. Geol. Soc. 166 (4), 601–616.
Geissler, W.H., Gaina, C., Hopper, J.R., Funck, T., Blischke, A., Arting, U., á Horni, J., Péron-Pinvidic, G., Abdelmalak, M.M., 2017. Seismic volcanostratigraphy of the NE Greenland continental margin. Geological Society, London, Special Publications 447 (1), 149–170.
Geoffroy, L., 2005. Volcanic passive margins. Compt. Rendus Geosci. 337 (16), 1395–1408.
Geoffroy, L., Burov, E.B., Werner, P., 2015. Volcanic passive margins: another way to break up continents. Sci. Rep. 5 (1), 1–12.
Gernigon, L., Blischke, A., Nasuti, A., Sand, M., 2015. Conjugate volcanic rifted margins, seafloor spreading, and microcontinent: insights from new high-resolution aeromagnetic surveys in the Norway Basin. Tectonics 34 (5), 907–933.
Gladczenko, T.P., Skogseid, J., Eldhom, O., 1998. Namibia volcanic margin. Mar. Geophys. Res. 20 (4), 313–341.
Greene, J.A., Tominaga, M., Miller, N.C., Hutchinson, D.R., Karl, M.R., 2017. Refining the formation and early evolution of the Eastern North American Margin: new insights from multiscale magnetic anomaly analyses. J. Geophys. Res.: Solid Earth 122 (11), 8724–8748.
Gunawardana, P.M., Moucha, R., Rooney, T.O., Stein, S., Stein, C.A., 2019. North America's Midcontinental Rift: a Coincidental Rendezvous of a Plume with a Rift. In Prep for Submission to Geology.
Hames, W.E., McHone, J.G., Ruppel, C., Renne, P. (Eds.), 2002. The Central Atlantic Magmatic Province: insights from fragments of Pangea. American Geophysical. Union Monograph 136, p. 267.
Harkin, C., Kusznir, N., Roberts, A., Manatschal, G., Horn, B., 2020. Origin, composition and relative timing of seaward dipping reflectors on the Pelotas rifted margin. Mar. Petrol. Geol. 114, 104235.
Heilman, E., Kolawole, F., Atekwana, E.A., Mayle, M., 2019. Controls of basement fabric on the linkage of rift segments. Tectonics 38 (4), 1337–1366.
Hill, J.C., Brothers, D.S., Hornbach, M.J., Sawyer, D.E., Shillington, D.J., Bécel, A., 2018. Subsurface Controls on the Development of the Cape Fear Slide Complex, Central US Atlantic Margin, vol. 477. Geological Society, London, Special Publications. SP477-17.
Holbrook, W.S., Kelemen, P.B., 1993. Large igneous province on the US Atlantic margin and implications for magmatism during continental breakup. Nature 364 (6436), 433.
Holbrook, S., Talwani, M., 1994. Seismic structure of the U.S. Mid-Atlantic continental margin. J. Geophys. Res. 99 (B9), 17871–17891.
Huismans, R., Beaumont, C., 2011. Depth-dependent extension, two-stage breakup and cratonic underplating at rifted margins. Nature 473, 74–78.
Keen, C.E., Stockmal, G.S., Welsink, H., Quinlan, G., Mudford, B., 1987. Deep crustal structure and evolution of the rifted margin northeast of Newfoundland: results from LITHOPROBE East. Can. J. Earth Sci. 24 (8), 1537–1549.
Kelemen, P.B., Holbrook, W.S., 1995. Origin of thick, high-velocity igneous crust along the US East Coast Margin. J. Geophys. Res.: Solid Earth 100 (B6), 10077–10094.
King, S.D., Anderson, D.L., 1995. An alternative mechanism of flood basalt formation. Earth Planet Sci. Lett. 136 (3–4), 269–279.
King, S.D., 2007. Hotspots and edge-driven convection. Geology 35 (3), 223–226.
Koopmann, H., Brune, S., Franke, D., Breuer, S., 2014. Linking rift propagation barriers to excess magmatism at volcanic rifted margins. Geology 42 (12), 1071–1074.
Koptev, A., Cloetingh, S., Burov, E., François, T., Gerya, T., 2017. Long-distance impact of Iceland plume on Norway's rifted margin. Sci. Rep. 7 (1), 10408.
Lundin, E.R., Redfield, T., Péron-Pindivic, G., 2014. Rifted Continental Margins: Geometric Influence on Crustal Architecture and Melting *from* Sedimentary Basins: Origins, Depositional Histories, and Petroleum Systems, pp. 1–36. Pindell, J., Horn, B., Rosen, N., Weimer, P, Dinkleman, M., Lowrie, A., Fillon, R., Granath, J. and Kennan, L. (auths) 33.
Lundin, E.R., Doré, A.G., Redfield, T.F., 2018. Magmatism and extension rates at rifted margins. Petrol. Geosci. 24 (4), 379–392.
Maguire, P.K.H., Keller, G.R., Klemperer, S.L., Mackenzie, G.D., Keranen, K., Harder, S., O'Reilly, B., Thybo, H., Asfaw, L., Khan, M.A., Amha, M., 2006. In: Yirgu, G., Ebinger, C.J., Maguire, P.K.H. (Eds.), Crustal Structure of the Northern Main Ethiopian Rift from the EAGLE Controlled-Source Survey; a Snapshot of Incipient Lithospheric Break-Up *from* the Afar Volcanic Province within the East African Rift System, vol. 259, pp. 269–291.
Marzoli, A., Renne, P.R., Piccirillo, E.M., Ernesto, M., Bellieni, G., De Min, A., 1999. Extensive 200 million-year-old continental flood basalts of the Central Atlantic Magmatic Province. Science 284, 616–618.

McDermott, C., Lonergan, L., Collier, J.S., McDermott, K.G., Bellingham, P., 2018. Characterization of seaward-dipping reflectors along the South American Atlantic margin and implications for continental breakup. Tectonics 37 (9), 3303–3327.
McHone, J.G., 2000. Non-plume magmatism and tectonics during the opening of the central Atlantic Ocean. Tectonophysics 316, 287–296.
McHone, J.G., 2020. Igneous Features and Geodynamic Models of Rifting and Magmatism Around the Central Atlantic Ocean. *http://www.mantleplumes.org/CAMP.html*.
Menzies, M.A., Klemperer, S.L., Ebinger, C.J., Baker, J., 2002. Characteristics of Volcanic Rifted Margins. Special Papers-Geological Society of America, pp. 1–14.
Mjelde, R., Kasahara, J., Shimamura, H., Kamimura, A., Kanazawa, T., Kodaira, S., Raum, T., Shiobara, H., 2002. Lower crustal seismic velocity-anomalies; magmatic underplating or serpentinized peridotite? Evidence from the Vøring Margin, NE Atlantic. Mar. Geophys. Res. 23 (2), 169–183.
Molnar, N.E., Cruden, A.R., Betts, P.G., 2018. Unzipping continents and the birth of microcontinents. Geology 46 (5), 451–454.
Morgan, R.L., Watts, A.B., 2018. Seismic and gravity constraints on flexural models for the origin of seaward dipping reflectors. Geophys. J. Int. 214 (3), 2073–2083.
Morgan, W.J., 1981. 13. Hotspot tracks and the opening of the Atlantic and Indian Oceans. The oceanic lithosphere 7, 443.
Morgan, W.J., 1983. Hotspot tracks and the early rifting of the Atlantic. In: Developments in Geotectonics, vol. 19. Elsevier, pp. 123–139.
Müller, R.D., Cannon, J., Qin, X., Watson, R.J., Gurnis, M., Williams, S., Pfaffelmoser, T., Seton, M., Russell, S.H.J., Zahirovic, S., 2018. GPlates: building a virtual Earth through deep time. G-cubed 19, 2243–2261.
Müller, R.D., Gaina, C., Roest, W.R., Hansen, D.L., 2001. A recipe for microcontinent formation. Geology 29 (3), 203–206.
Mueller, C.O., Jokat, W., 2017. Geophysical evidence for the crustal variation and distribution of magmatism along the central coast of Mozambique. Tectonophysics 712, 684–703.
Mutter, J.C., Detrick, R.S., North Atlantic Transect Study Group, 1984. Multichannel seismic evidence for anomalously thin crust at Blake Spur fracture zone. Geology 12 (9), 534–537.
Neely, J.S., Stein, S., Merino, M., Adams, J., 2018. Have we seen the largest earthquakes in eastern North America? Phys. Earth Planet. In. 284, 17–27.
Norcliffe, J.R., Paton, D.A., Mortimer, E.J., McCaig, A.M., Nicholls, H., Rodriguez, K., Hodgson, N., van der Spuy, D., 2018. Laterally Confined Volcanic Successions (LCVS); recording rift-jumps during the formation of magma-rich margins. Earth Planet Sci. Lett. 504, 53–63.
Paton, D.A., Pindell, J., McDermott, K., Bellingham, P., Horn, B., 2017. Evolution of seaward-dipping reflectors at the onset of oceanic crust formation at volcanic passive margins: insights from the South Atlantic. Geology 45 (5), 439–442.
Planke, S., Eldholm, O., 1994. Seismic response and construction of seaward dipping wedges of flood basalts: Vøring volcanic margin. J. Geophys. Res.: Solid Earth 99 (B5), 9263–9278.
Reuber, K., Mann, P., 2019. Control of Precambrian-to-Paleozoic orogenic trends on along-strike variations in Early Cretaceous continental rifts of the South Atlantic ocean. Interpretation 7 (4), 1–80.
Reuber, K., Mann, P., Pindell, J., 2019. Hotspot origin for asymmetrical conjugate volcanic margins of the austral South Atlantic Ocean as imaged on deeply-penetrating seismic reflection images. Interpretation 7 (4), 1–88.
Richards, M.A., Duncan, R.A., Courtillot, V.E., 1989. Flood basalts and hot-spot tracks: plume heads and tails. Science 246 (4926), 103–107.
Roberts, D.G., Bally, A.W., 2012. Some remarks on basins and basin classification and tectonostratigraphic megasequences. In: Regional Geology and Tectonics: Principles of Geologic Analysis. Elsevier, pp. 76–92.
Rooney, T.O., Lavigne, A., Svoboda, C., Girard, G., Yirgu, G., Ayalew, D., Kappelman, J., 2017. The making of an underplate: pyroxenites from the Ethiopian lithosphere. Chem. Geol. 455, 264–281.
Ruppel, C., 1995. Extensional processes in continental lithosphere. J. Geophys. Res.: Solid Earth 100 (B12), 24187–24215.
Saria, E., Calais, E., Altamimi, Z., Willis, P., Farah, H., 2013. A new velocity field for Africa from combined GPS and DORIS space geodetic solutions, contribution to the definition of the African reference frame. AFREF: *J. Geophys. Res.* 118, 1677–1697.
Soares, D.M., Alves, T.M., Terrinha, P., 2012. The breakup sequence and associated lithospheric breakup surface: their significance in the context of rifted continental margins (West Iberia and Newfoundland margins, North Atlantic. Earth Planet Sci. Lett. 355, 311–326.
Schiffer, C., Peace, A., Phethean, J., Gernigon, L., McCaffrey, K., Petersen, K.D., Foulger, G., 2018. The Jan Mayen Microplate Complex and the Wilson Cycle, vol. 470. Geological Society, London, Special Publications, pp. 393–414.
Schnabel, M., Franke, D., Engels, M., Hinz, K., Neben, S., Damm, V., Grassmann, S., Pelliza, H., Dos Santos, P.R., 2008. The structure of the lower crust at the Argentine continental margin, South Atlantic at 44°S. Tectonophysics 454 (1–4), 14–22.
Schneider, C.A., Rasband, W.S., Eliceiri, K.W., 2012. NIH Image to ImageJ: 25 years of image analysis. Nat. Methods 9 (7), 671–675.
Schulte, S.M., Mooney, W.D., 2005. An updated global earthquake catalogue for stable continental regions: reassessing the correlation with ancient rifts. Geophys. J. Int. 161 (3), 707–721.
Sengor, A.M.C., Burke, K., 1978. Relative timing of rifting and volcanism on Earth and its tectonic implications. Geophys. Res. Lett. 5 (6), 419–421.
Senkans, A., Leroy, S., d'Acremont, E., Castilla, R., Despinois, F., 2019. Polyphase rifting and break-up of the central Mozambique margin. Mar. Petrol. Geol. 100, 412–433.
Sheridan, R.E., Musser, D.L., Glover III, L., Talwani, M., Ewing, J.I., Holbrook, W.S., Purdy, G.M., Hawman, R., Smithson, S., 1993. Deep seismic reflection data of EDGE US mid-Atlantic continental-margin experiment: implications for Appalachian sutures and Mesozoic rifting and magmatic underplating. Geology 21 (6), 563–567.
Shudofsky, G.N., Cloetingh, S., Stein, S., Wortel, R., 1987. Unusually deep earthquakes in East Africa: constraints on the thermo-mechanical structure of a continental rift system. Geophys. Res. Lett. 14 (7), 741–744.
Stein, S., Sleep, N.H., Geller, R.J., Wang, S.C., Kroeger, G.C., 1979. Earthquakes along the passive margin of eastern Canada. Geophys. Res. Lett. 6 (7), 537–540.
Stein, S., Cloetingh, S., Sleep, N.H., Wortel, R., 1989. Passive margin earthquakes, stresses and rheology. In: Earthquakes at North-Atlantic Passive Margins: Neotectonics and Postglacial Rebound. Springer, Dordrecht, pp. 231–259.
Stein, C.A., Kley, J., Stein, S., Hindle, D., Keller, G.R., 2015. North America's Midcontinent Rift: when rift met LIP. Geosphere 11 (5), 1607–1616.
Stein, S., Stein, C.A., Elling, R., Kley, J., Keller, G.R., Wysession, M., Rooney, T., Frederiksen, A., Moucha, R., 2018a. Insights from North America's failed Midcontinent Rift into the evolution of continental rifts and passive continental margins. Tectonophysics 744, 403–421.
Stein, C.A., Stein, S., Elling, R., Keller, G.R., Kley, J., 2018b. Is the "Grenville Front" in the central United States really the Midcontinent Rift? GSA Today (Geol. Soc. Am.) 28 (5), 4–10.
Stein, S., Wysession, M., 2003. An Introduction to Seismology, Earthquakes, and Earth Structure. John Wiley & Sons.
Svartman Dias, A.E., Lavier, L.L., Hayman, N.W., 2015. Conjugate rifted margins width and asymmetry: the interplay between lithospheric strength and thermomechanical processes. J. Geophys. Res.: Solid Earth 120, 8672–8700.
Thybo, H., Artemieva, I.M., 2013. Moho and magmatic underplating in continental lithosphere. Tectonophysics 609, 605–619.
Tian, X., Buck, W.R., 2019. Lithospheric thickness of volcanic rifting margins: constraints from seaward dipping reflectors. J. Geophys. Res.: Solid Earth 124 (4), 3254–3270.
Ten Brink, U.S., Chaytor, J.D., Geist, E.L., Brothers, D.S., Andrews, B.D., 2014. Assessment of tsunami hazard to the US Atlantic margin. Mar. Geol. 353, 31–54.
Tréhu, A.M., Ballard, A., Dorman, L.M., Gettrust, J.F., Klitgord, K.D., Schreiner, A., 1989. Structure of the lower crust beneath the Carolina Trough, US Atlantic continental margin. J. Geophys. Res.: Solid Earth 94 (B8), 10585–10600.
Tugend, J., Gillard, M., Manatschal, G., Nirrengarten, M., Harkin, C., Epin, M.E., Sauter, D., Autin, J., Kusznir, N., McDermott, K., 2018. Reappraisal of the Magma-Rich versus Magma-Poor Rifted Margin Archetypes, vol. 476. Geological Society, London, Special Publications, pp. SP476–S479.
van Wijk, J.W., Huismans, R.S., Ter Voorde, M., Cloetingh, S.A.P.L., 2001. Melt generation at volcanic continental margins: no need for a mantle plume? Geophys. Res. Lett. 28 (20), 3995–3998.
van Wijk, J.W., Van der Meer, R., Cloetingh, S.A.P.L., 2004. Crustal thickening in an extensional regime: application to the mid-Norwegian Vøring margin. Tectonophysics 387 (1–4), 217–228.
Vervoort, J.D., Wirth, K., Kennedy, B., Sandland, T., Harpp, K.S., 2007. The magmatic evolution of the Midcontinent rift: new geochronologic and geochemical evidence from felsic magmatism. Precambrian Res. 157 (1–4), 235–268.
White, R., McKenzie, D., 1989. Magmatism at rift zones: the generation of volcanic continental margins and flood basalts. J. Geophys. Res.: Solid Earth 94 (B6), 7685–7729.
White, R.S., Spence, G.D., Fowler, S.R., McKenzie, D.P., Westbrook, G.K., Bowen, A.N., 1987. Magmatism at rifted continental margins. Nature 330 (6147), 439.
White, R.S., Smith, L.K., Roberts, A.W., Christie, P.A.F., Kusznir, N.J., 2008. Lower-crustal intrusion on the North Atlantic continental margin. Nature 452 (7186), 460.
Wolin, E., Stein, S., Pazzaglia, F., Meltzer, A., Kafka, A., Berti, C., 2012. Mineral, Virginia, earthquake illustrates seismicity of a passive-aggressive margin. Geophys. Res. Lett. 39 (2).
Zwaan, F., Corti, G., Keir, D., Sani, F., 2020. A review of tectonic models for the rifted margin of Afar: implications for continental break-up and passive margin formation. J. Afr. Earth Sci. 164, 103649.